Available online at www.sciencedirect.com

SciVerse ScienceDirect

Ceramics International 39 (2013) 1977–1983

CERAMICS INTERNATIONAL

www.elsevier.com/locate/ceramint

Temperature dependent structural and dielectric investigations of $PbZr_{0.5}Ti_{0.5}O_3$ solid solution at the morphotropic phase boundary

Geetika Srivastava*, Ankur Goswami, A.M. Umarji

Materials Research Centre, Indian Institute of Science, Bangalore 560012, India

Received 8 May 2012; received in revised form 17 August 2012; accepted 17 August 2012
Available online 23 August 2012

Abstract

$PbZr_{1-x}Ti_xO_3$ ceramics synthesised by low temperature calcination followed by sintering at 1280 °C show a Morphotropic Phase Boundary (MPB) for compositions of $x=0.44$–0.51. The morphotropic phase boundary is wider for samples with smaller grain sizes due to the synthesis route. A Rietveld analysis is performed on a composition of $x=0.5$ composition to quantify the phase fractions of the tetragonal and monoclinic phases present in the PZT system. Temperature dependent X-ray diffraction and dielectric studies of $PbZr_{0.5}Ti_{0.5}O_3$ composition demonstrated a phase transformation from monoclinic to tetragonal at 270 °C followed by a ferroelectric tetragonal to a paraelectric cubic transition at 370 °C. Thus, the poling of these ceramics should be performed below 270 °C to benefit from the presence of a monoclinic phase.

Keywords: A. Sintering; B. Grain size; C. Dielectric properties; D. PZT

1. Introduction

Solid solutions of $PbZr_{1-x}Ti_xO_3$ (PZT) are an important class of ferroelectric materials that have been widely investigated due to their remarkable dielectric and piezoelectric properties [1]. These materials exhibit excellent dielectric, elastic and piezoelectric properties [2,3] at the 'Morphotropic Phase Boundary (MPB), the term coined by Jaffe, Cook and Jaffe [2]. This MPB in the PZT system was long believed to separate the two phases namely, the Ti rich tetragonal (T) phase and the Zr rich rhombohedral (R) phase.

Numerous studies have reported the optimal composition and width of this MPB region. The MPB was previously reported to be a region of coexistence for the two phases [4–8], and the width of the region is believed to be affected by compositional heterogeneity and sample processing techniques [9,10]. Soares et al. and Cao and Cross attempted to explain the width of this coexistence region using a statistical distribution model and found an inverse relationship between Δx and the grain size of the ceramics [8,11].

While the origin of the exceptional properties in this region has already been investigated in detail by many authors, it remains a topic of debate [9]. The best accepted explanation for the enhanced properties of PZT ceramics at the MPB is related to the increased ease of the polarisation reorientation during poling. The tetragonal phase provides six possible orientations of polarisation along the pseudo-cubic $\langle 001 \rangle$ direction, while the rhombohedral features eight available polarisations directions along the $\langle 111 \rangle$ directions. Thus, the coexistence of phases, at the MPB leads to nearly degenerate energies, providing 14 possible polarisation directions [10]. However, the recent discovery of a stable monoclinic phase by Noheda et al. using the synchrotron x-ray powder diffraction measurements disproved the earlier hypothesis that the rhombohedral and tetragonal phases coexist in the MPB region. This landmark discovery provided a new perspective on the nature of the MPB and suggested a different explanation for the extreme properties in this region [11–13].

The original composition–temperature (x–T) phase diagram of the PZT system proposed by Jaffe, Cook and Jaffe [2] was modified by Noheda et al. [11] to include the monoclinic phase in the system.

*Corresponding author. Present address: Department of Physics and Materials Science and Engineering, Jaypee Institute of Information Technology, Noida 201307, India. Tel.: +91 120 2594386 (office); fax: +91 120 2400986.
E-mail address: geetika.srivastava@jiit.ac.in (G. Srivastava).

0272-8842/$ - see front matter © 2012 Elsevier Ltd and Techna Group S.r.l. All rights reserved.
http://dx.doi.org/10.1016/j.ceramint.2012.08.049

The unit cell in the monoclinic phase is twice the volume of the tetragonal phase and has b as its unique axis. In this phase, $\boldsymbol{a}_m$ and $\boldsymbol{b}_m$ lie along the tetragonal $[\bar{1}\bar{1}0]$ and $[\bar{1}\bar{1}0]$ directions, and $\boldsymbol{c}_m$ is slightly tilted away from the [001] direction such that the angle β between $\boldsymbol{a}_m$ and $\boldsymbol{c}_m$ is slightly greater than 90°. The polar axis of this monoclinic phase is directed anywhere within the monoclinic ac plane thus, the polar axis is free to rotate within this plane. Bellaiche [14] concluded that the monoclinic phase forms a transitional bridge between the tetragonal and rhombohedral phases and accounts for the continuous change in the polarisation direction from the [001] tetragonal to the [111] rhombohedral directions as the distance away from the MPB increases. Hence, high piezoelectric coefficients and larger electromechanical responses are observed experimentally.

The existence of a monoclinic phase in the temperature–composition (x–T) phase diagram of the PZT-type systems has been the subject of intense debate in the recent years. Ragini et al. carried out a detailed Rietveld analysis and found that in the MPB region, the tetragonal (P4mm) and monoclinic phases (Cm) coexist [15–17]. Singh et al. found that the so-called 'rhombohedral phase' of the Zr-rich composition is a monoclinic phase [18].

Therefore, it is valuable to investigate the temperature dependence of the phase of MPB composition as there is a strong correlation between the structure of the system and its material properties. Therefore, to account for the exceptional material properties observed at the MPB, it is necessary to perform a detailed and systematic structural study of the system. As the Zr/Ti ratio plays an important role in the phase change of the system [19], detailed structural investigations of the coexistence region in $PbZr_{1-x}Ti_xO_3$ for $x=0.40$–0.54 compositions have been performed using X-ray diffraction. The goal of this study is to lower the grain sizes of the samples to broaden the MPB. This broadening is needed to enhance the material properties of the system by adopting a low calcination synthesis route [20,21]. Furthermore an MPB for compositions from $x=0.44$ to 0.51. Hence, a high resolution diffraction study was performed on a sample with a composition of $x=0.5$ revealing almost equal proportions of tetragonal and monoclinic phases. A temperature dependent structural study was also performed on $x=0.5$ by HT XRD. Dielectric measurements were also carried out to confirm the phase transition in the system as observed through X-ray diffraction. The purpose of this investigation is to determine the phase fraction of the tetragonal and monoclinic phases in the coexistence region, and to study the phase transformation in the solid solution of PZT along with the evolution of cell parameters with respect to temperature. This information may elucidate the material properties exhibited by the system in the coexistence region.

2. Experimental details

The nominal composition of $PbZr_{1-x}Ti_xO_3$ ($x=0.40$–0.54) was synthesised using a low temperature calcination route. The samples were prepared by a two-step solid-state reaction using PbO, ZrO_2 (Fluka, 99% purity) and TiO_2 (s.d. fine chem. ltd. of 99.5% purity) in a stoichiometric ratio. The reactant powders were calcined at 700 °C for 1 h, pelletised and later sintered in a controlled lead atmosphere at 1280 °C for 2 h. The morphological features of the fractured surface of the sintered ceramics coated with gold were studied by scanning electron microscopy (Cambridge Stereoscan S360). The electrical properties such as dielectric constant, dielectric loss of the sintered pellets have been measured using HP – 4194A impedance/gain-phase analyzer. The capacitance and dielectric loss were measured in the frequency range 100 Hz to 100 KHz from room temperature to 723 K. The rate of heating was maintained at 2 K/min for the measurement.

The pellets were crushed using an agate mortar and pestle to pass through a 38 μm sieve. High resolution X-ray diffraction data were recorded in the 2θ range from 10° to 120°at a 0.017° step size using an AXS Bruker D8 ADVANCE with Cu K_α radiation. For non-ambient studies, the diffractometer was equipped with a basic chamber consisting of an effective, uniformly heating radiant heater, with an indirectly heated sample carrier capable of rotation. The sample slurry was prepared with ethanol and spread uniformly on a Ta heating foil, the temperature of which was monitored by an S-type thermocouple. The temperature profile of the sample was maintained at a constant heating rate of 5 °C/min.

3. Rietveld refinement details

The high resolution X-ray diffraction data were processed by the Rietveld refinement using the programme FULLPROF 2006 [22]. The background was fit using the linear interpolation method. The structure was refined according to the following sequence. The scale factor was refined first, followed by the zero point of the detector, the lattice constants and the atomic positions. Later, the peak shape and asymmetric parameters were also introduced. The peak profile was chosen as pseudo-voigt. The occupational parameters of the ions were kept fixed during the refinement. The anisotropic thermal parameters were taken into account for the Pb atom whereas the remaining atoms were refined using isotropic thermal parameters. Finally, the thermal parameters of individual atoms were refined.

The structural model developed here was based on the coexistence of monoclinic and tetragonal phases for the $PbZr_{0.5}Ti_{0.5}O_3$ composition. The space group of the tetragonal phase of PZT is P4mm at room temperature, with Pb^{2+} in 1(a) sites at (0,0,0), Zr^{4+}/Ti^{4+} and O_I^{2-} in 1(b) sites at (0.5, 0.5, z) and O_{II}^{2-} in 2(c) sites at (0.5, 0, z). The space group of the monoclinic phase for the structural model is taken as Cm, as has been reported previously by several authors. The monoclinic system consists of four ions in the asymmetric unit Pb^{2+} at (0, 0, 0), Zr^{4+}/Ti^{4+} and O_I^{2-} occupying 2(a) sites at (x, 0, z) and O_{II}^{2-} occupying 4(b) sites at (x, y, z). The initial structural parameters for the refinement of the monoclinic and tetragonal phases were taken from Ragini et al [17]. Table 1 summarises the starting

Table 1
The starting model used for the structural refinement of $PbZr_{0.5}Ti_{0.5}O_3$.

	Monoclinic phase			Tetragonal phase		
	x	*y*	*z*	*x*	*y*	*z*
Pb^{2+}	0	0	0	0	0	0
Zr^{4+}/Ti^{4+}	0.5	0.5	*z*	*x*	0	*z*
O_I^{2-}	0.5	0.5	*z*	0.5	0	*z*
O_{II}^{2-}	0.5	0	*z*	*x*	*y*	*z*
***a* (Å)**	4.04			5.76		
***b* (Å)**	4.04			5.74		
***c* (Å)**	4.13			4.08		
***β* (deg.)**	–			90.50		

model. The initial values of the lattice parameters for the refinement were obtained by the least square method using the PROSZKI programme [23]. The isotropic thermal parameter for Pb^{2+} was attempted in the initial refinement, but the anisotropic thermal parameter yielded a better fit with an improved *R* value. Thus, the anisotropic thermal parameter for Pb^{2+} was used in the refinement.

4. Results and discussions

As stated above, PZT ceramics with compositions in the MPB are generally preferred due to the exceptional material properties in this coexistence region, which makes them technologically important for sensors and actuators. However, the literature reports various compositions and widths of the coexistence region due to the processing techniques and conditions employed by various authors, as discussed earlier. Thus, a systematic XRD study was carried out on the PZT system by varying the Zr/Ti ratio.

Fig. 1 plots the diffraction patterns for the PZT compositions under study in the 2θ range 35–55°. Fig. 1 shows that a (200) pseudocubic peak is split into two peaks for an $x=0.48$ composition, a signature of the tetragonal phase in the system. For the PZT compositions in the present study, the composition $x=0.5$ was chosen because clear splitting of the (200) pseudocubic peak into three peaks was observed at this composition. The system moves away from the MPB when the Zr content is increased. Thus, the composition of the PZT system under investigation was fixed at $x=0.5$.

4.1. Rietveld refinement of the structure of $PbZr_{0.5}Ti_{0.5}O_3$

The quantitative phase analysis of the tetragonal and monoclinic phases was carried out by performing a Rietveld refinement of the structure of the PZT system.

Fig. 2 depicts the observed, calculated and difference profiles of the refined structure at room temperature. The observed diffraction profile is represented by red dots. The continuous black line represents the diffraction profile calculated using the structural model. The difference

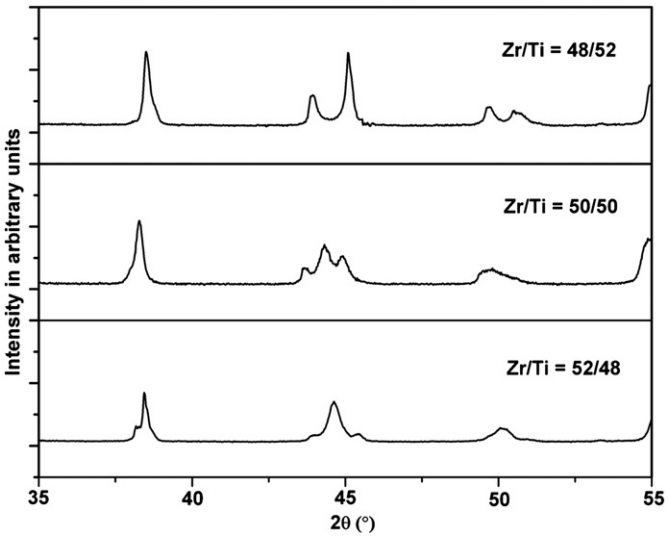

Fig. 1. The diffraction patterns for various compositions of the PZT system.

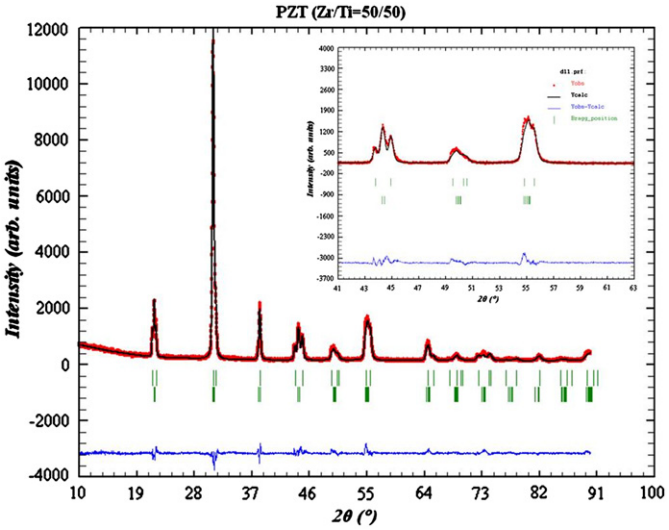

Fig. 2. Observed, calculated and difference profiles for a Rietveld refined structure of $PbZr_{0.5}Ti_{0.5}O_3$ at room temperature. The inset shows an expanded view of the structural refinement in the 2θ range of 40°–60°. (For interpretation of the references to colour in this figure, the reader is referred to the web version of this article.)

between the observed and calculated profile is indicated by a continuous blue line. The upper green bars represent the Bragg reflection positions for the tetragonal phase, whereas the lower green bars represent the Bragg reflection positions for the monoclinic phase for Cu K_α radiation. The positions of the peaks are very well described by the presence of monoclinic and tetragonal phases as seen from the Bragg reflection positions for the two phases.

The best fit criterion in a Rietveld refinement is the difference profile obtained after a satisfactory refinement has been achieved. Generally, the *R*-factor weighted profile R_{wp}, the statistically expected R_{exp} and the goodness of fit

indices χ^2 determine the quality of the fit, adequacy and accuracy of the assumed model.

This model seems to provide a satisfactory fit as shown by the difference profile and the χ^2 value of 3.33. The inset of Fig. 2 shows an expanded plot of the structural fitting of the PZT system in the 2θ range between 40°and 60°. The fit of the triplet splitting of the (200) reflection clearly demonstrates good refinement. The satisfactory fit of these reflections validate the model.

The reliability factors of R_{wp} and R_{exp} were found to be 14.4% and 7.91% respectively through iterative refinement after the best fit between the observed and calculated pattern was achieved. The obtained *R*-factors were found to be in the acceptable range.

To facilitate comparison, the equivalent perovskite cell parameters a_m and b_m for the monoclinic phase are calculated from the monoclinic cell parameters A_m and B_m by the following relation:

$$a_m = \frac{A_m}{\sqrt{2}}, \quad b_m = \frac{B_m}{\sqrt{2}}$$

The c/a ratio is defined in the case of the monoclinic phase by the relation

$t_m = 2\sqrt{2}c_m/(A_m + B_m)$ to correspond to the c_t/a_t value of the tetragonal phase.

The lattice cell parameters of the two phases are determined by a careful Rietveld profile fitting procedure for the coexistence region. Table 2 reports the structural details determined by the refinement.

The weight fraction of the monoclinic phase was found to be 58% with the remaining weight fraction (i.e. 42%) representing the tetragonal phase in the $PbZr_{0.5}Ti_{0.5}O_3$ solid solution.

4.2. High temperature X-ray diffraction profile of $PbZr_{0.5}Ti_{0.5}O_3$

4.2.1. Phase transformation in the PZT system with a variation in temperature

Fig. 3 shows the X-ray diffraction patterns of the PZT system from $2\theta = 35^\circ$ to 60° as the temperature is varied from 25 °C to 370 °C. The lattice planes reflections were examined to estimate the phase transition temperature. The lattice plane reflections show large changes as temperature is increased with the peak profiles evolving toward pseudocubic reflections. The room temperature X-ray diffraction profile indicates a coexistence region (MPB) composed of two phases, a monoclinic phase and a tetragonal phase. The triplet splitting of the (200) pseudocubic reflection becomes a singlet peak as temperature is increased clearly marking the phase transition from ferroelectric to paraelectric. The MPB transforms to a pseudocubic phase via an intermediate phase of tetragonal phase.

The peaks become narrower as the temperature increases, and the PZT system finally transforms to a pseudocubic phase at approximately 370 °C. The transition from the tetragonal to the cubic phase occurs between 350 °C and 370 °C. The structure is cubic above this temperature confirmed by the fact that the reflections have the same Full Width at Half Maximum (FWHM) above this temperature.

The phase transformation of the MPB region to a pure tetragonal phase occurs between 200 °C and 300 °C which can be explained by the tilting behaviour of the MPB region in the phase diagram of PZT as suggested by Jaffe, Cook and Jaffe, later modified by Noheda et al. and then revised by Ragini et al. [2,12,17]. Dielectric measurements were carried out to confirm the phase transformation. Fig. 4 shows the variation of the dielectric constant and dielectric loss. A slight bump is

Table 2
The Rietveld refined structural parameters of $PbZr_{0.5}Ti_{0.5}O_3$ system (at MPB) for tetragonal and monoclinic phases.

	Tetragonal phase				**Monoclinic phase**			
	x	***y***	***z***	***U* (Å²)**	***x***	***y***	***z***	***U* (Å²)**
Pb^{2+}	0	0	0	$U_{11}=U_{22}=0.011(5)$ $U_{33}=0.067(4)$	0	0	0	$U_{11}=0.2168(4)$ $U_{22}=0.0225(1)$ $U_{33}=0.0704(4)$ $U_{13}=0.0256(2)$
Zr^{4+}/Ti^{4+}	0.5	0.5	0.466(3)	0.007(1)	0.435(3)	0	0.525(4)	0.011(3)
O_I^{2-}	0.5	0.5	−0.077(8)	0.009(2)	0.5	0	0.116(9)	0.004(2)
O_{II}^{2-}	0.5	0	0.369(4)	0.012(1)	0.195(6)	0.232(8)	0.567(9)	0.036(3)
***a* (Å)**	4.0339(3)				5.773(1)			
***b* (Å)**	4.0339(3)				5.752(1)			
***c* (Å)**	4.1373(3)				4.095(1)			
β	–				90.44(1)			
***c/a* Ratio**	1.026				1.004			
% Molar	58				42			
R_B	5.29				6.00			
R_{wp}	14.4							
R_{exp}	7.91							
χ^2	3.33							

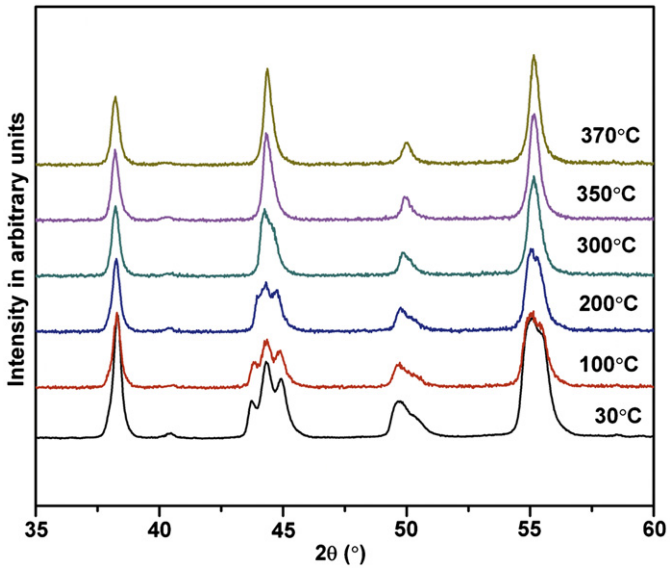

Fig. 3. The variation of XRD profiles with temperatures from room temperature to 500 °C.

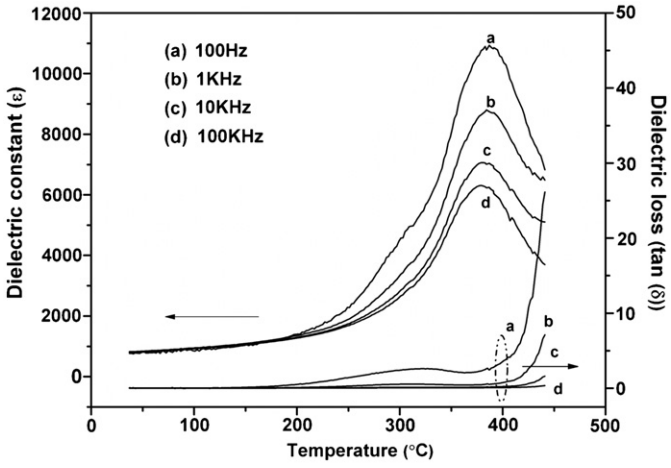

Fig. 4. The variation of dielectric properties with temperature.

observed at approximately 290–300 °C indicating that a phase transformation occurrs in the system in this temperature range presumably to a tetragonal phase. The modified phase diagram by Noheda et al. [11] demonstrates that if the temperature of the PZT system in the MPB region is increased, the system first transforms to a tetragonal phase and then to a cubic phase. This bump in the dielectric constant was previously shown to originate from the rhombohedral (now proved to be monoclinic)-tetragonal transition by hot stage XRD results [24,25] and was also observed by Deng et al. [26]. The phase transformation to the pseudocubic phase occurs at approximately 370 °C as shown by the data analysis on the X-ray diffraction profiles of the PZT system with varying temperatures. However, the dielectric measurement showed a transition temperature, T_c, of 384 °C. The phase transformations from monoclinic to tetragonal and from tetragonal to a paraelectric cubic phase are clearly seen by

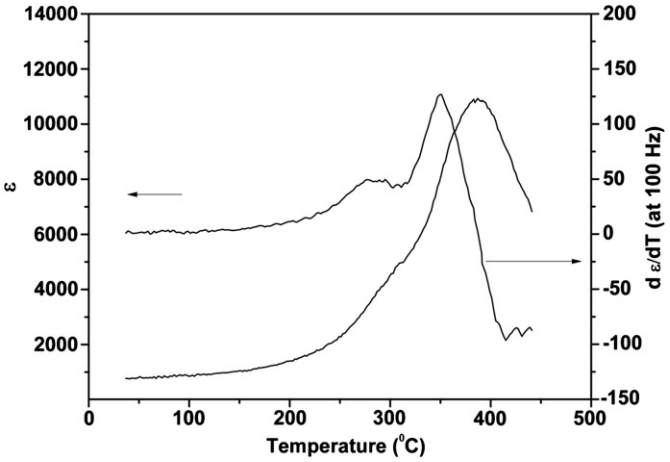

Fig. 5. The derivative plot of dielectric permittivity at 100 Hz with temperature.

plotting the derivative of the dielectric permittivity with respect to temperature, as shown in Fig. 5.

4.2.2. Variation in the lattice parameters with change in temperature

Fig. 6 shows the trend in the lattice parameters after refinement of the monoclinic, tetragonal and pseudocubic phases of the PZT system with respect to the temperature. This figure shows that as temperature is increased, the lattice parameter c_t of the tetragonal phase strongly decreases while the lattice parameter a_t increases slightly and approaches its value in the cubic phase. The lattice parameters of the monoclinic phase also tend toward the lattice parameter of the cubic phase as temperature is increased. The $\angle\beta$ varies from 90.44° to 90.27° for the monoclinic phase which coexists with the tetragonal phase from room temperature (25 °C) to 200 °C. The lattice parameter of the cubic phase, which appears at >370 °C is almost constant. The errors in the lattice parameters are found to be within 5%. The lattice parameter of the cubic phase, which exists above 370 °C is 4.065 ± 0.002 Å. These results show that as the temperature is increased, the system transforms to the cubic phase.

4.3. Grain size effect

Soares et al. explain the width of the region of coexistence of the phases via a model of the statistical distribution of phases. This model shows that the width of the coexistence region (Δx) is related to the grain size [27]. This model was found to be in good agreement with the experimental results obtained by this group. Further, Cao and Cross attempted to model the width of this coexistence region based on the difference in the free energy of the two phases and found that an inverse relationship exists between the coexistence region and the grain size of the system [28–30].

Kakegawa et al. [31] and Mabud [32] observed that Δx depends on the sintering temperature and time, which in fact govern the grain size of the sample. Thus, by varying the

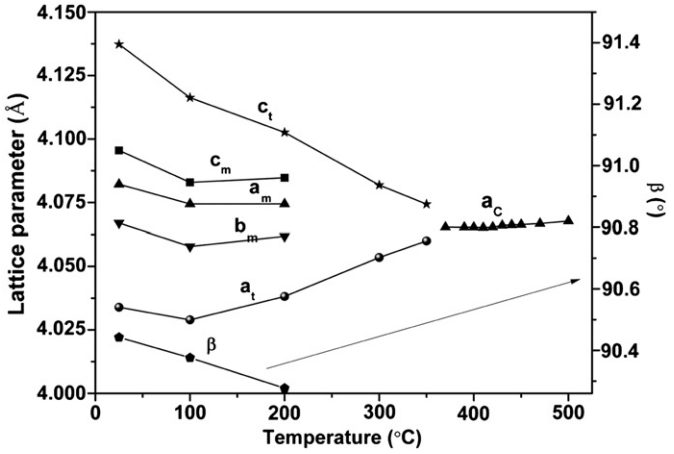

Fig. 6. The temperature dependence of lattice parameters as obtained from the X-ray diffraction data.

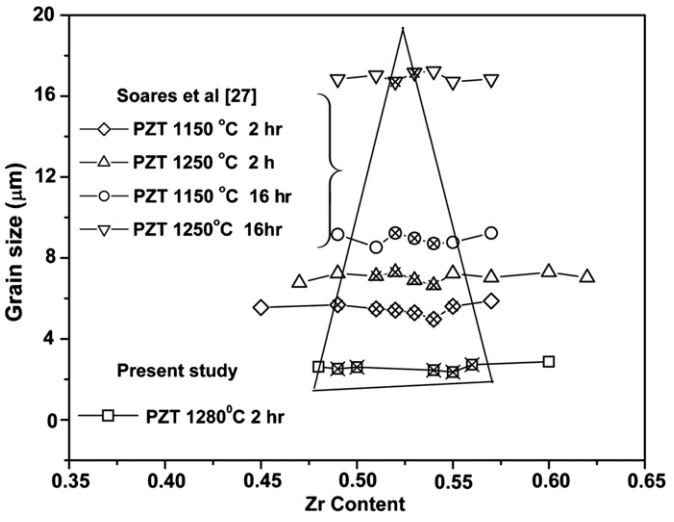

Fig. 7. The effect of grain size on the coexistence region of PZT.

sintering temperature and time, Soares et al. were able to synthesise samples of $PbZr_{1-x}Ti_xO_3$ (PZT) with compositions in the range $0.38 \leq x \leq 0.55$. The sintering temperature and time were varied to obtain different grain sizes. Based on their observations, they attempted to validate the inverse relationship between the width of the coexistence region and the grain size of the synthesised samples. The PZT data were taken from the work of Soares et al. [27]. The samples synthesised using our novel synthesis are marked with squares.

The reactant powders were calcined at 700 °C followed by sintering at 1280 °C. The phase evolution of lead-based perovskite has previously been studied and discussed in detail by our coworkers [20]. Calcination above 700 °C led to the formation of a predominantly $A_3B_4O_{13}$ pyrochlore phase (along with a PbO phase and a perovskite phase). This pyrochlore phase is highly stable and thus, is not completely eliminated during the sintering stage. However, calcination of the reactant powders at 700 °C results in the formation of an $A_3B_2O_8$ type of pyrochlore. The formation of a perovskite phase is known to be a result of the diffusion of B-site cations into B-site deficient pyrochlores such as the $A_3B_2O_8$ lattice. Hence, once the $A_3B_4O_{13}$ pyrochlore phase is formed, further B-site cation diffusion does not occur, making it difficult to revert to the perovskite phase is difficult.

Thus, it is necessary for the $A_3B_2O_8$ type pyrochlore to form during the calcination stage so that a pyrochlore-free perovskite phase can be formed after sintering. The additional advantage of this low calcination approach is the formation of fine particles (< 1 μm) that help to reduce the sintering temperature. Hence, this work attempts to achieve a pure perovskite phase via the stabilisation of an intermediate, $A_3B_4O_{13}$ pyrochlore phase between 600 °C and 700 °C.

This new approach of low calcination followed by sintering yielded samples with grain sizes of approximately 1–2 μm. The grain sizes were estimated using the SigmaScan Pro 4.0 software with several test lines drawn on the SEM image. The average grain size was determined using the linear intercept method [33]. Fig. 7 shows the dependence of the mean grain size in sintered ceramics for the PZT system. The cross (x) denotes the coexistence region of the system. The broadening of the coexistence region with decreasing grain size is indicated by the triangle marked in Fig. 7. The samples synthesised by the low temperature calcination route yielded a smaller grain size, which resulted in broadening of the coexistence region. A similar relationship was observed for solid solutions of $y\text{PZT}-(1-y)\text{PZN}$ ($y=0.1$ and 0.2) synthesised by the low temperature calcination route [20,21].

5. Conclusions

Lead-based ceramics were synthesised using a low temperature calcination route. This method broadened the width of the MPB region due to the smaller grain size. This wider MPB is needed to improve the performance of these materials at the device level.

High resolution X-ray studies show that the MPB consists of a monoclinic Zr-rich phase and a tetragonal Ti-rich phase at room temperature, and the proportions of these phases have been quantified. The evolution of the lattice parameters of the system with respect to the temperature was also studied. The MPB region transforms from mixed phases to a tetragonal and finally to a pseudocubic phase as the temperature is increased. The dielectric properties show the signature of the phase transformation. Hence, to gain full advantage of the monoclinic phase, the MPB samples should be poled below 270 °C.

References

[1] A. Safari, E.K. Akdoğan, Piezoelectric and Acoustic Materials for Transducers Applications, Springer, New York, 2008.
[2] B. Jaffe, W.R. Cook Jr., H. Jaffe, Piezoelectric Ceramics, Academic Press, London, UK, 1971.

[3] Z. Ye, Handbook of advanced, dielectric, piezoelectric and ferroelectric materials: synthesis, properties and applications CRC, Boca Raton, 2008.
[4] A. Boutarfaia, Investigations of co-existence region in lead zirconate–titanate solid solutions: X-ray diffraction studies, Ceramics International 26 (2000) 583–587.
[5] J. Joseph, T.M. Vimala, V. Sivasubramanian, V.R.K. Murthy, Structural investigations on $Pb(Zr_xT_{1-x})O_3$ solid solutions using the X-ray Rietveld method, Journal of Materials Science 35 (2000) 1571–1575.
[6] J.C. Fernandes, D.A. Hall, M.R. Cockburn, G.N. Greaves, Phase coexistence in PZT ceramic powders, Nuclear Instruments and Methods in Physics Research Section B: Beam Interactions with Materials and Atoms 97 (1995) 137–141.
[7] A.S. Bhalla, R. Guo, E.F. Alberta, Some comments on the morphotropic phase boundary and property diagrams in ferroelectric relaxor systems, Materials Letters 54 (2002) 264–268.
[8] M.R. Soares, A.M.R. Senos, P.Q. Mantas, Phase coexistence region and dielectric properties of PZT ceramics, Journal of the European Ceramic Society 20 (2000) 321–334.
[9] R. Guo, L.E. Cross, S.E. Park, B. Noheda, D.E. Cox, G. Shirane, Origin of the high piezoelectric response in $PbZr_{1-x}Ti_xO_3$, Physical Review Letters 84 (2000) 5423–5426.
[10] R. Waser, U. Böttger, S. Tiedke, Polar oxides: properties, characterization, and imaging, Wiley-VCH Verlag GmbH & Co. KGaA, 2005.
[11] B. Noheda, D.E. Cox, G. Shirane, J.A. Gonzalo, L.E. Cross, S.E. Park, A monoclinic ferroelectric phase in the $Pb(Zr_{1-x}Ti_x)O_3$ solid solution, Applied Physics Letters 74 (1999) 2059–2061.
[12] B. Noheda, J.A. Gonzalo, L.E. Cross, R. Guo, S.E. Park, D.E. Cox, G. Shirane, Tetragonal-to-monoclinic phase transition in a ferroelectric perovskite: the structure of $PbZr_{0.52}Ti_{0.48}O_3$, Physical Review B 61 (2000) 8687–8695.
[13] D.E. Cox, B. Noheda, G. Shirane, Low-temperature phases in $PbZr_{0.52}Ti_{0.48}O_3$: a neutron powder diffraction study, Physical Review B 71 (2005) 134110.
[14] L. Bellaiche, A. Garcia, D. Vanderbilt, Finite-temperature properties of $Pb(Zr_{1-x}Ti_x)O_3$ alloys from first principles, Physical Review Letters 84 (2000) 5427.
[15] D.M. Hatch, H.T. Stokes, R. Ranjan, Ragini, S.K. Mishra, D. Pandey, B.J. Kennedy, Antiferrodistortive phase transition in $Pb(Ti_{0.48}Zr_{0.52})O_3$: space group of the lowest temperature monoclinic phase, Physical Review B 65 (2002) 212101.
[16] R. Ranjan, A.K. Singh, Ragini, D. Pandey, Comparison of the Cc and R3c space groups for the superlattice phase of $Pb(Zr_{0.52}Ti_{0.48})O_3$, Physical Review B 71 (2005) 092101.
[17] Ragini, R. Ranjan, S.K. Mishra, D. Pandey, Room temperature structure of $Pb(Zr_xTi_{1-x}O_3)$ around the morphotropic phase boundary region: a Rietveld study, Journal of Applied Physics 92 (2002) 3266–3274.
[18] A.K. Singh, D. Pandey, S. Yoon, S. Baik, N. Shin, High-resolution synchrotron x-ray diffraction study of Zr-rich compositions of $Pb(Zr_xTi_{1-x})O_3$ ($0.525 <= x <= 0.60$): evidence for the absence of the rhombohedral phase, Applied Physics Letters 91 (2007) 192903–192904.
[19] Y. Yan, K.-H. Cho, S. Priya, Identification and effect of secondary phase in MnO_2-doped $0.8Pb(Zr_{0.52}Ti_{0.48})O_3$–$0.2Pb(Zn_{1/3}Nb_{2/3})O_3$ piezoelectric ceramics, Journal of the American Ceramic Society 94 (2011) 3953–3959.
[20] Geetika, A.M. Umarji, The influence of Zr/Ti content on the morphotropic phase boundary in the PZT–PZN system, Materials Science and Engineering, B—Advanced Functional Solid-State Materials 167 (2010) 171–176.
[21] V.V. Bhat, B. Angadi, A.M. Umarji, Synthesis, low temperature sintering and property enhancement of PMN–PT ceramics based on the dilatometric studies, Materials Science and Engineering, B—Advanced Functional Solid-State Materials 116 (2005) 131–139.
[22] L.M.D. Cranswick, Winplotr Graphics and Fullprof Rietveld (and Single Crystal) Software, 〈http://www.ccp14.ac.uk/tutorial/fullprof/wininst.html〉.
[23] W. Lasocha, K. Lewinski, PROSZKI—a system of programs for powder diffraction data analysis, Journal of Applied Crystallography 27 (1994) 437–438.
[24] G. Robert, M. Demartin, D. Damjanovic, Phase diagram for the $0.4Pb(Ni_{1/3},Nb_{1/3})O_3$–$0.6Pb(Zr,Ti)O_3$ solid solution in the vicinity of a morphotropic phase boundary, Journal of the American Ceramic Society 81 (1998) 749–753.
[25] X.P. Jiang, J.W. Fang, H.R. Zeng, G.R. Li, D.R. Chen, Q.R. Yin, Dielectric properties of $Pb(Zn_{1/3}Nb_{2/3})O_3$–$PbZrO_3$–$PbTiO_3$ system in the rhombohedral region near the morphotropic phase boundary, Journal of Materials Research 15 (2000) 2745–2749.
[26] G. Deng, A. Ding, X. Zheng, W.Q. Yin, Phase diagram for the $0.3Pb(Zn_{1/3}Nb_{2/3})O_3$–$0.7Pb_{0.96}La_{0.04}(ZrTi)_{0.99}O_3$ solid solution in the vicinity of morphotropic phase boundary, Journal of Physics D—Applied Physics 38 (2005) 2452–2459.
[27] M.R. Soares, A.M.R. Senos, P.Q. Mantas, Phase coexistence in PZT ceramics, Journal of the European Ceramic Society 19 (1999) 1865–1871.
[28] W. Cao, L.E. Cross, Theoretical model for the morphotropic phase boundary in lead zirconate & #150; lead titanate solid solution, Physical Review B 47 (1993) 4825–4830.
[29] W. Cao, L.E. Cross, Distribution functions of coexisting phases in a complete solid solution system, Journal of Applied Physics 73 (1993) 3250–3255.
[30] W. Cao, L.E. Cross, The ratio of rhombohedral and tetragonal phases on the morphotropic phase boundary in lead zirconate titanate, Japanese Journal of Applied Physics 31 (1992) 1399–1402.
[31] K. Kakegawa, J. Mohri, T. Takahashi, H. Yamamura, S. Shirasaki, A compositional fluctuation and properties of $Pb(Zr,Ti)O_3$, Solid State Communications 24 (1977) 769–772.
[32] S.A. Mabud, The morphotropic phase boundary in PZT solid solutions, Journal of Applied Crystallography 13 (1980) 211–216.
[33] M.I. Mendelson, Average grain size in polycrystalline ceramics, Journal of the American Ceramic Society 52 (1969) 443–446.